Available online at www.sciencedirect.com

ScienceDirect

www.elsevier.com/locate/jes

JES JOURNAL OF ENVIRONMENTAL SCIENCES

www.jesc.ac.cn

Investigation of $PM_{2.5}$ pollution during COVID-19 pandemic in Guangzhou, China

Luyao Wen[1], *Chun Yang*[1], *Xiaoliang Liao*[1], *Yanhao Zhang*[2], *Xuyang Chai*[1], *Wenjun Gao*[3], *Shulin Guo*[1], *Yinglei Bi*[1], *Suk-Ying Tsang*[4], *Zhi-Feng Chen*[1], *Zenghua Qi*[1,*], *Zongwei Cai*[1,2,*]

[1] *Guangdong-Hong Kong-Macao Joint Laboratory for Contaminants Exposure and Health, School of Environmental Science and Engineering, Institute of Environmental Health and Pollution Control, Guangdong University of Technology, Rm 510, Engineering Facility Building No.3, Guangzhou 510006, China*

[2] *State Key Laboratory of Environmental and Biological Analysis, Department of Chemistry, Hong Kong Baptist University, Hong Kong, China*

[3] *Guangzhou Meteorological Public Service Center, Guangzhou Meteorological Service, Guangzhou 510006, China*

[4] *School of Life Sciences, The Chinese University of Hong Kong, Hong Kong, China*

ARTICLE INFO

Article history:
Received 19 April 2021
Revised 29 June 2021
Accepted 7 July 2021
Available online 15 July 2021

Keywords:
$PM_{2.5}$ pollution
COVID-19 pandemic
$PM_{2.5}$ composition
Meteorological analysis
Source appointment

ABSTRACT

The COVID-19 pandemic has raised awareness about various environmental issues, including $PM_{2.5}$ pollution. Here, $PM_{2.5}$ pollution during the COVID-19 lockdown was traced and analyzed to clarify the sources and factors influencing $PM_{2.5}$ in Guangzhou, with an emphasis on heavy pollution. The lockdown led to large reductions in industrial and traffic emissions, which significantly reduced $PM_{2.5}$ concentrations in Guangzhou. Interestingly, the trend of $PM_{2.5}$ concentrations was not consistent with traffic and industrial emissions, as minimum concentrations were observed in the fourth period (3/01-3/31, 22.45 $\mu g/m^3$) of the lockdown. However, the concentrations of other gaseous pollutants, e.g., SO_2, NO_2 and CO, were correlated with industrial and traffic emissions, and the lowest values were noticed in the second period (1/24-2/03) of the lockdown. Meteorological correlation analysis revealed that the decreased $PM_{2.5}$ concentrations during COVID-19 can be mainly attributed to decreased industrial and traffic emissions rather than meteorological conditions. When meteorological factors were included in the $PM_{2.5}$ composition and backward trajectory analyses, we found that long-distance transportation and secondary pollution offset the reduction of primary emissions in the second and third stages of the pandemic. Notably, industrial $PM_{2.5}$ emissions from western, southern and southeastern Guangzhou play an important role in the formation of heavy pollution events. Our results not only verify the importance of controlling traffic and industrial emissions, but also provide targets for further improvements in $PM_{2.5}$ pollution.

* Corresponding authors.
E-mails: zenghuaqi@gdut.edu.cn (Z. Qi), zwcai@hkbu.edu.hk (Z. Cai).

https://doi.org/10.1016/j.jes.2021.07.009

Introduction

Guangzhou, with a permanent population of over 15.3 million in 2019 (Guangzhou Statistics Bureau, 2020), is a national central city and an international trade hub. Annual $PM_{2.5}$ concentrations in Guangzhou decreased from 52.0 $\mu g/m^3$ in 2013 to 23.0 $\mu g/m^3$ in 2020, yet still exceed WHO Air Quality Guidelines (annual mean: 10 $\mu g/m^3$) (Guangzhou Municipal Ecological Environment Bureau, 2020). Moreover, the Guangdong-Hong Kong-Macao Greater Bay Area (GBA) has the worst air quality, including $PM_{2.5}$ pollution, of the world's four major bay areas. On the premise of maintaining rapid economic growth, an accurate analysis of $PM_{2.5}$ sources is critical for further improvements to the air quality in Guangzhou.

At the start of the COVID-19 pandemic, nationwide restrictive measures, such as stay-at-home recommendations, travel bans, cessation of public transportation, and the closing of shopping centers and entertainment venues, provided a unique opportunity to explore the dynamics and sources of $PM_{2.5}$ contamination. This was done by comparing changes in $PM_{2.5}$ concentrations and composition during different periods of the COVID-19 pandemic (Liu et al., 2020; Lv et al., 2020; Tanzer-Gruener et al., 2020). The degree of local $PM_{2.5}$ contamination is determined by meteorological conditions, long-range transportation and atmospheric chemistry, as well as local emissions, with these factors exerting synergistic effects on $PM_{2.5}$ pollution (An et al., 2019; Chen et al., 2020b; Wang et al., 2015; Zhao et al., 2013). The dramatic decrease in anthropogenic emissions, such as industrial and traffic emissions, during the COVID-19 lockdown greatly reduced the complexity of $PM_{2.5}$ sources. This made it easier to accurately identify $PM_{2.5}$ sources, as well as their relative contribution to pollution episodes. Nevertheless, unexpected heavy $PM_{2.5}$ pollution, also termed "pandemic haze", was observed in several Chinese cities and regions, especially the Beijing-Tianjin-Hebei region (BTH), during different stages of the COVID-19 pandemic (Chang et al., 2020; Huang et al., 2021; Lv et al., 2020; Zhao et al., 2020b).

The pillar industries of GBA are mainly light industries such as electronics, electrical machinery and petrochemical industry; For this reason, the $PM_{2.5}$ concentrations and composition in Guangzhou differ significantly from other regions in China, i.e., lower concentrations but a larger organic fraction (Chen et al., 2020a; Liao et al., 2021). Over the past year, numerous reports have analyzed $PM_{2.5}$ contamination profiles, formation mechanisms and sources during the COVID-19 lockdown through various methods, e.g., satellite remote sensing, online monitoring, and mathematical models. These studies have focused on clarifying the inorganic components of $PM_{2.5}$, e.g., sulfate, nitrate, and ammonium (SNA), elemental carbon (EC), and crustal elements (CM) (Chang et al., 2020; Ghahremanloo et al., 2021; Li et al., 2020; Liu et al., 2020; Lv et al., 2020; Tanzer-Gruener et al., 2020). However, changes in the $PM_{2.5}$ pollution levels in Guangzhou, especially those concerning the organic fraction, were rarely analyzed due to a lack of samples representing different phases of the COVID-19 pandemic.

In this study, main air pollutants ($PM_{2.5}$, CO, SO_2, NO_2, and O_3) and meteorological conditions were traced in Guangzhou from 13 January to 30 April 2020, which were divided into five distinct periods according to the epidemic process. We quantitatively investigated the specific effects of both industrial and traffic emissions reduction due to COVID-19 lockdown and the variation of meteorological conditions on $PM_{2.5}$ contamination in Guangzhou, a modern city based on the light industry in southern China. Furthermore, we tried to clarify the potential sources in Guangzhou based on the mass and composition of $PM_{2.5}$ particles collected during the COVID-19 lockdown and backward trajectory analyses, with an emphasis on the heavy pollution cases. Our results can provide both targets and regulation strategies for further improvements in $PM_{2.5}$ pollution.

1. Materials and methods

1.1. *Sample and data collection*

$PM_{2.5}$ sampling campaigns were conducted in the Guangzhou Higher Education Mega Center (HEMC, 23.04°N, 113.37°E), which is a relatively independent area surrounded by the Pearl River. This sampling site was selected because of the following factors: (1) HEMC is located in the main city zone of Guangzhou and is thus representative of the local air quality; (2) heavy industrial and serious traffic emissions do not exist at the HEMC; therefore, the samples were assumed to reflect overall urban air conditions. Two medium-volume air samplers (Laoying Co. Ltd., Qingdao, China) with Quartz microfiber filters (Whatman, QMA, 90 mm diameter) were used to collect samples over 24 hr at a flow rate of 100 L/min. In this study, 24 $PM_{2.5}$ samples were collected during the COVID-19 outbreak (8 samples/month) for quantitative analyses.

Data concerning local air pollutants ($PM_{2.5}$, SO_2, NO_2, CO and O_3) and meteorological conditions including temperature, relative humidity, rainfall, solar radiation, wind direction, wind speed and planetary boundary layer height (PBLH) were obtained from monitoring stations in HEMC, which was 1 km away from $PM_{2.5}$ sampling site, established by the Guangzhou Municipal Ecological Environment Agency and Guangzhou Meteorological Service.

The traffic flow is based on the statistics of 9 key toll stations in Guangzhou. Public traffic refers to the number of passengers on public transport. The statistics from the website of Guangzhou Municipal Transport Bureau (http://jtj.gz.gov.cn/jtzt/jtsj/jtysyb/index.html). The data of gross output value and added value of industrial enterprises above designated size in Guangzhou was obtained from the website of Guangzhou Bureau of Statistics. (http://112.94.72.17/portal/queryInfo/macroReport/economicSituationIndex).

1.2. *Time period setting*

Quantifying changes in air quality during the COVID-19 lockdown requires precisely defined time periods that enable comparisons of spatiotemporal variations in $PM_{2.5}$ concentrations. The studied period was from January 13, 2020 to April 30, 2020. The COVID-19 epidemic in Guangdong province began on January 23 and the First-Level Public Health Emergency Response was initiated, which lasted until February 23. And then the emergency response to the novel coronavirus epidemic was

Table 1 – Division of the COVID-19 epidemic in Guangzhou into distinct time periods.

Time period	COVID-19 epidemic	Corresponding time period in 2019	Information about the period
COVID-19 I	1/13-1/22	1/25-2/3	Before Chinese New Year Vacation and COVID-19 lockdown
COVID-19 II	1/23-2/03	2/04-2/10	Chinese New Year Vacation
COVID-19 III	2/04-2/29	2/11-2/28	Primary emergency response to the novel coronavirus epidemic
COVID-19 IV	3/01-3/31	3/01-3/31	Secondary emergency response to the novel coronavirus epidemic
COVID-19 V	4/01-4/30	4/01-4/30	After COVID-19 lockdown

lowered to the second level. By the end of March, the resumption rate of work and production of industrial enterprises above the scale in Guangdong Province was over 99% and the industrial production has basically returned to normal. Detailed information was summarized in Table S1. Considering the two factors of the local investigation in Guangzhou and Chinese New Year Vacation (CNY), we have divided the epidemic process into five distinct time periods (COVID-19 I to V, detailed in Table 1), and determined the corresponding time periods in 2019.

1.3. $PM_{2.5}$ composition analysis

$PM_{2.5}$ constituents were characterized according to a previously described methodology (Qi et al., 2020; Zhang et al., 2019). Water soluble inorganic ions, 16 Environmental Protection Agency (EPA) polycyclic aromatic hydrocarbons (PAHs), crustal elements (CM), organic carbon (OC) and elemental carbon (EC) were measured in the collected $PM_{2.5}$ samples during the COVID-19 epidemic. At first, the extraction of eight water-soluble inorganic ions (K^+, Ca^{2+}, Na^+, Mg^{2+}, Cl^-, $SO_4{}^{2-}$, $NO_3{}^-$, $NH_4{}^+$) was operated by the ultrasonic method. Quartz microfiber filters with $PM_{2.5}$ samples were fixed in a glass bottle with 15 mL ultrapure water and then took the ultrasound for 20 min with low temperature. After centrifuge, the supernatant was measured by ion chromatography (Aquion, Thermo Scientific, USA) to determine the concentrations of inorganic ions.

Sixteen priority PAHs, including naphthalene (Nap), acenaphthene (Ace), acenaphthylene (Acy), fluorene (Flu), phenanthrene (Phe), anthracene (Ant), fluoranthene (Flt), pyrene (Pyr), benz[a]anthracene (BaA), chrysene (Chr), benzo[b]fluoranthene (BbF), benzo[k]fluoranthene (BkF), Benzo[a]pyrene (BaP), indeno[1,2,3–cd]pyrene (IcdP), dibenz[a,h]anthracene (DahA), and benzo[ghi]perylene (BghiP) were extracted, concentrated, and analyzed. The analysis was operated on a TSQ 8000 Evo gas chromatograph mass spectrometer (Thermo Scientific, USA) equipped with a Thermo TRACE™1300 gas chromatograph, an electron ionization (EI) source, triple quadrupole analyzer and automatic injector (GC-EI-MS/MS). A Thermo TG-5MS capillary column (Thermo Scientific, USA) was applied to the separation.

The temperature program for the oven was as follows: the initial temperature of 80 °C was maintained for 1 min, and then increased to 180 °C at a rate of 5 °C/min (maintained for 2 min); the temperature continued increasing to 240 °C at a rate of 2.5 °C/min and was eventually increased to 300 °C at 3 °C/min and held for 1 min. The injections were splitless, and the sample volume was 1 μL. High-purity helium was used as the carrier gas at a constant flow rate of 1 mL/min. The temperature of the injector, ion source and transfer line were set at 280, 250 and 280 °C, respectively. Quantitative analysis was conducted on selected ion monitoring (SIM) mode. The chromatograph peaks of the samples were identified by mass spectra and retention time.

Inductively coupled plasma mass spectrometer (ICP-MS, 7700X; Agilent Technologies, Santa Clara, California, USA) was used to determine the elemental compositions of the collected samples on filters, including Na, Mg, Al, K, Ca, Ti, V, Cr, Ni, Mn, Fe, Ba, Cu, Zn, As and Pb. Carbonaceous aerosol components, OC and EC, were quantified using a Desert Research Institute (DRI) Model 2001 carbon analyzer (Atmoslytic Inc., Calabasas, CA, USA). The IMPROVE-A thermal/optical reflectance (TOR) protocol was used for the analyses (Chow et al., 2007; Wu et al., 2018).

1.4. Source appointment

The PAH diagnostic ratio represents a semi-quantitative way to identify sources of PAHs and the usefulness of PAH isomer ratios in source identification has been extensively proved (Dong et al., 2021; Le et al., 2020; Lu et al., 2017; Xu et al., 2020a). The diagnostic ratios of Ant/(Phe + Ant), Flt/(Flt + Pyr), IcdP/(IcdP + BghiP), and BaA/(BaA + Chr) were calculated to investigate the sources of $PM_{2.5}$-bound PAHs during COVID-19 III to V (Table S2). The ratio of Ant/(Phe + Ant) $<$0.1 indicates the source of petroleum, while a ratio $>$ 0.1 indicates a dominance of combustion(i.e. combustion of organic matter, anthropogenic industrial activities, or natural fire). Moreover, a ratio of Flt/(Flt + Pyr) $<$ 0.4 stands for the petrogenic sources, 0.4–0.5 for petroleum combustion (especially liquid fossil fuel, vehicle and crude oil), while $>$ 0.5 for combustion of biomass and coal. Ratios of IcdP/(IcdP + BghiP) $<$ 0.2 and BaA/(BaA + Chr) $<$ 0.20 indicate a petroleum source. Ratios of BaA/(BaA + Chr) of 0.20–0.35 and IcdP/(IcdP + BghiP) of 0.20–0.50 indicated origin of PAHs from petroleum combustion (liquid fossil fuel, vehicle, and crude oil combustion). If IcdP/(IcdP + BghiP) $>$0.50 and BaA/(BaA + Chr) $>$ 0.50, the PAHs originated from coal, grass, and wood.

The air-mass backward trajectories were calculated and clustered to track the transport pathways of airflow arriving in HEMC (23.04°N, 113.37°E) using the Hybrid Single Particle Lagrangian Integrated Trajectory (HYSPLIT) model. The 72 hr backward trajectories started at 0:00 (UTC) for three distinct pandemic haze events (PEs) and were calculated at 500 m above ground level (AGL) using meteorological data

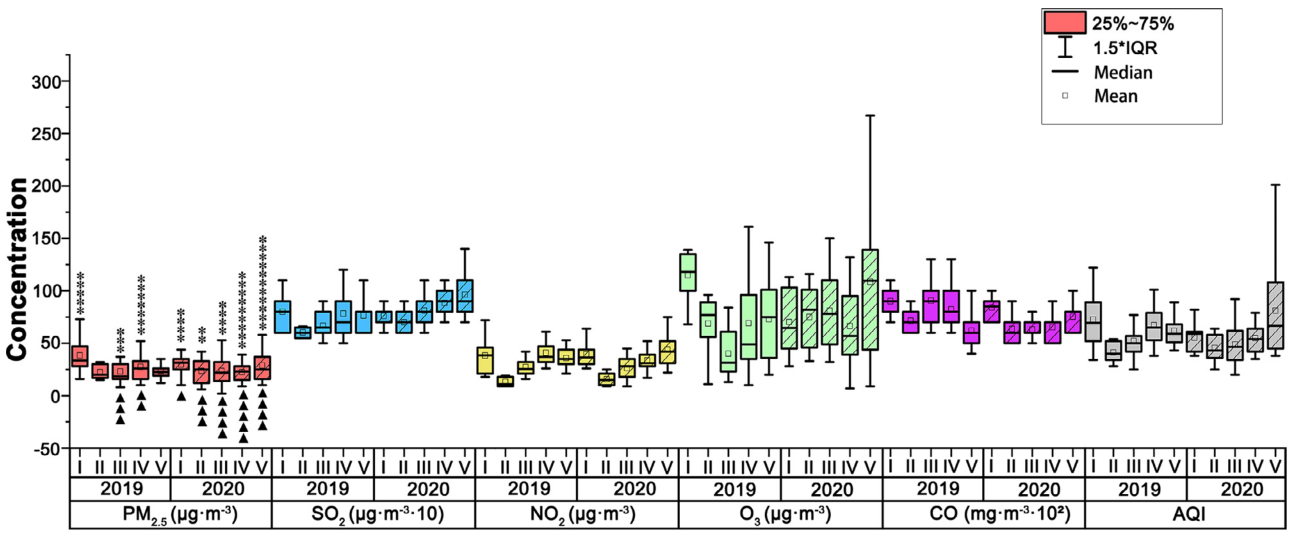

Fig. 1 – Changes in the concentration of AQI and five air pollutants during the COVID-19 lockdown and corresponding periods of 2019 in Guangzhou. * and ▲ represent events with $PM_{2.5}$ concentrations above 35 $\mu g/m^3$ and below 12 $\mu g/m^3$, respectively.

available at the National Oceanic and Atmospheric Administration (NOAA) Global Data Assimilation System (GDAS).

1.5. Statistical analysis

Air pollutant concentrations ($PM_{2.5}$, SO_2, NO_2, CO and O_3) and meteorological conditions were expressed as a daily average value. The wind direction used in this study is the main wind direction of the day in question. The significance of differences between spatial and temporal changes in pollutant concentrations were determined using an unpaired Student's *t*-test. Pearson's correlation coefficients were calculated in SPSS software (Version 26.0, Chicago, IL, USA) to determine the statistical significance of relationships between $PM_{2.5}$ pollution and meteorological parameters, with $p < 0.05$ set as the threshold for significance.

2. Results and discussion

2.1. Changes in air quality during the COVID-19 lockdown

Variations in the air quality of Guangzhou during different COVID-19 periods are shown in Fig. 1 and Table S3. SO_2, NO_2 and CO concentrations showed a V-shaped trend, i.e., an initial decrease followed by an increase, from period I to period V, with the lowest values occurring in period II (1/24-2/03, SO_2: 7.00 $\mu g/m^3$, NO_2: 15.64 $\mu g/m^3$, CO: 0.64 mg/m^3), which is consistent with industrial and traffic emissions. Due to the close relationship between anthropogenic emissions and air quality, we also investigated how the COVID-19 lockdown affected local industry and traffic. The gross output value of industrial enterprises and number of cars on the road showed minimum values in February, i.e., 23.1% and 71% decreases, respectively, from the same period in February 2019 (Fig. 2, Tables S4, S5). However, O_3 concentrations increased by 9.15%, to 102.12%, across periods II, III, and V; this result may be explained by the reduced NO_2 that hinders the reaction between NO and O_3, thus increasing the atmospheric oxidizing capacity (Le et al., 2020; Xu et al., 2020a). Furthermore, we found that O_3 slightly decreased in stage IV in 2020. This result could be attributed to the short sunshine duration, lower solar radiation, and higher relative humidity (Table S6), which were unfavorable to the formation and accumulation of O_3 (Bu et al., 2021; Mousavinezhad et al., 2021; Yin et al., 2019).

During the fifth stage (COVID-V), industrial and agricultural production, along with transportation levels, in most of China, including Guangdong Province, had almost returned to normal, which was reflected in a significant increase in air pollutant concentrations when compared to the corresponding period in 2019 and previous COVID-19 phases.

Across periods I to IV, the average and median $PM_{2.5}$ concentrations showed a downward trend, and the number of days with minimal $PM_{2.5}$ concentrations ($\leq$12 $\mu g/m^3$) increased. However, the degree to which $PM_{2.5}$ concentrations dropped was still far from expectations. When compared with industrial emission trends, the reduction in $PM_{2.5}$ concentrations showed a certain degree of lag. Notably, the unexpected increase in daily $PM_{2.5}$ mainly appeared in the BTH region, yet severe haze pollution was observed over eastern China during the COVID-19 shutdown (Chang et al., 2020; Huang et al., 2021; Lv et al., 2020; Zhao et al., 2020b). This high frequency of haze events with high $PM_{2.5}$ concentrations during the epidemic was mainly attributed to the higher secondary aerosol fraction of $PM_{2.5}$ caused by the unbalanced reduction of gaseous pollutants (NO_X, O_3 and VOCs) along with medium-scale regional transportation (Ghahremanloo et al., 2021; Huang et al., 2021; Jia et al., 2020; Lv et al., 2020; Shen et al., 2021). The variation in $PM_{2.5}$ concentrations over different regions during COVID-19 indicates that heavy industrial emissions are relevant to regional $PM_{2.5}$ pollution.

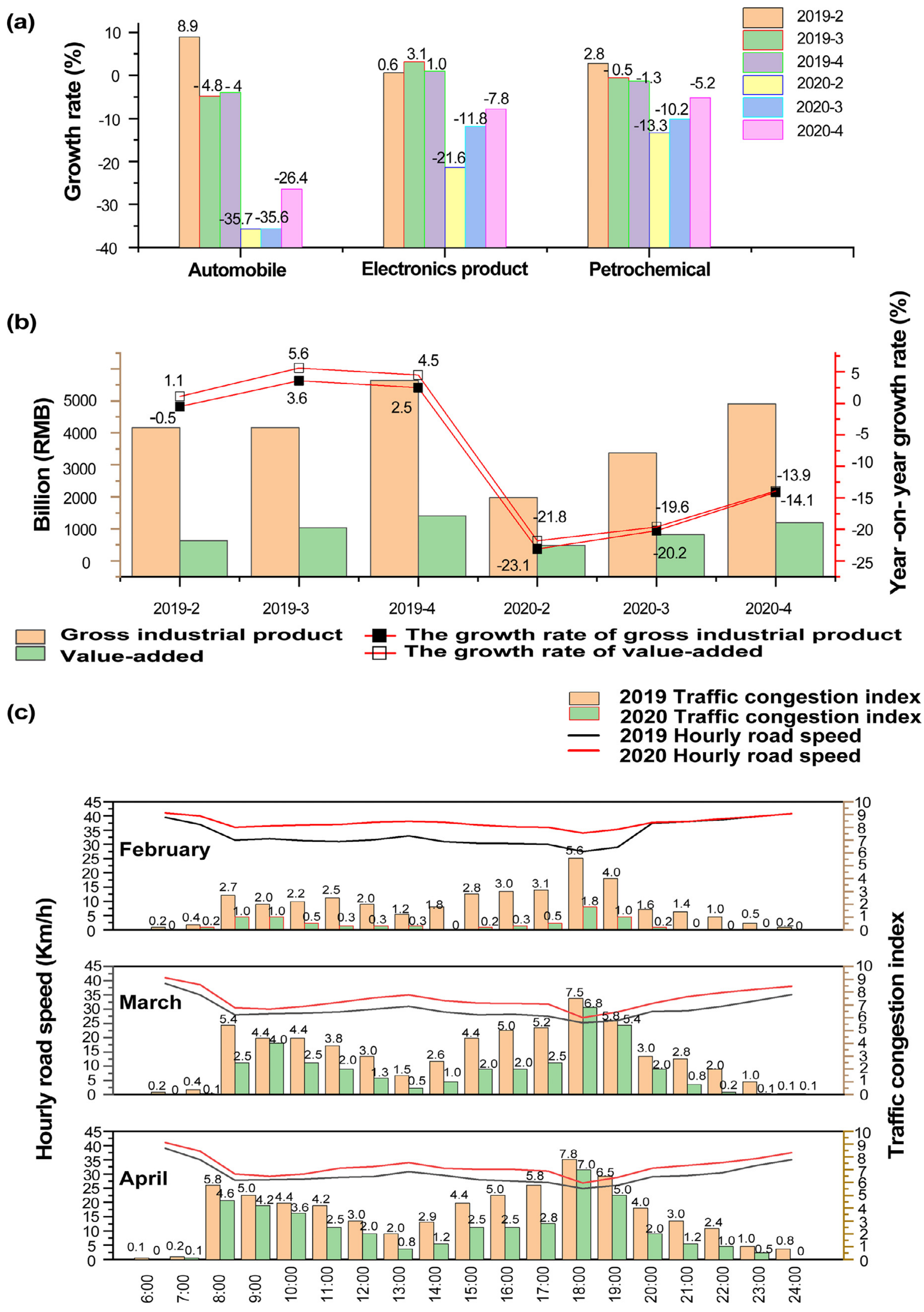

Fig. 2 – The variations of industry and traffic during the COVID-19 lockdown in Guangzhou. (a), (b) The total output value and the growth rate of the three pillar industries in Guangzhou compared with the same period last year, (c) traffic congestion index and hourly road speed (Km/hr) in 2020 compared with the corresponding periods of 2019 in Guangzhou. Traffic congestion index and hourly road speed (Km/hr) in 2020.

The conversion of gaseous pollutants into $PM_{2.5}$ through photochemical reactions can be extended to precursors of organic gases, such as sulfate and nitrate, which can be transformed into secondary particulate matter through a series of chemical reactions (Huang et al., 2014; Sun et al., 2016). Pearson correlation coefficients were calculated for average daily $PM_{2.5}$ and primary gas pollutant (CO, NO_2, SO_2, O_3) concentrations in Guangzhou across the studied COVID-19 phases. $PM_{2.5}$ and NO_2 showed the highest Pearson correlation coefficients (r = 0.68), followed by $PM_{2.5}$ and SO_2 (r = 0.63), O_3 (r= 0.53) and CO (r = 0.41) (Fig. S1). The correlation coefficients between $PM_{2.5}$ and gas pollutants during the COVID-19 shutdown were consistent with the values from previous years. However, the correlation coefficients between $PM_{2.5}$ and both NO_2 and SO_2 during periods I to III significantly increased relative to period V and the same period in 2019, which indicates that the formation of secondary $PM_{2.5}$ increased during the COVID-19 shutdown. In addition, the ratio of $PM_{2.5}$/CO (Table S7), an indicator of secondary pollutants to primary emissions, also increased during the COVID-19 shutdown, especially in period III. This further confirms the remarkable increase in the secondary aerosol fraction of $PM_{2.5}$ in Guangzhou during the COVID-19 pandemic.

2.2. Influence of meteorological conditions on $PM_{2.5}$ concentrations during the COVID-19 lockdown

Meteorological conditions impart a significant impact on $PM_{2.5}$ concentrations, mainly contributing to the diffusion, regional transportation, and secondary production of $PM_{2.5}$ (Chen et al., 2020b; Xu et al., 2020b). We first calculated Pearson correlation coefficients for $PM_{2.5}$ pollution and meteorological parameters to understand the mechanisms underlying the inconsistent reduction in anthropogenic emissions and $PM_{2.5}$ concentrations in Guangzhou. As shown in Fig. 3a, the wind speed had the strongest effect on $PM_{2.5}$ concentrations in Guangzhou during the COVID-19 epidemic (r = -0.56; p < 0.05), followed by daily total solar radiation, relative humidity, rainfall, PBLH and temperature. According to the rose diagrams and their relevant data of wind frequency- $PM_{2.5}$ and $PM_{2.5}$-wind speed-wind direction (Fig. 3b, Table S8), the occurrence frequency of southeast wind was the highest and $PM_{2.5}$ concentration was always maintained at a relatively high level (39.2–58.0 $\mu g/m^3$) when the southeast wind blows with the speed less than 2 m/sec, indicating that potential $PM_{2.5}$ emission sources may be existed in the southeast of the monitoring point. Additionally, southern and western winds showed stronger correlations with $PM_{2.5}$ pollution than winds from other directions (Fig. 3b, Table S8), which indicates that the observed $PM_{2.5}$ pollution may also come from these directions. We then compared certain meteorological parameters during the five tested COVID-19 periods and the corresponding time points of 2019 to investigate the extent to which meteorological conditions can explain the observed variations in $PM_{2.5}$ concentrations. Apparent differences in meteorological conditions were primarily explained by PBLH, relative humidity and temperature, both of which showed weak correlations with $PM_{2.5}$ concentrations (Fig. 3a, Table S6). Furthermore, We compared the meteorological data over the past five years and found no abnormal weather conditions during the COVID-19 epidemic, especially unfavorable meteorological conditions to $PM_{2.5}$ diffusion (Table S9). Thus, the decreased $PM_{2.5}$ concentrations during COVID-19 can be mainly attributed to decreased industrial and traffic emissions rather than meteorological conditions.

2.3. Composition analysis and source appointment of $PM_{2.5}$ in Guangzhou

PAHs, which originate from various emission sources, are one of the most abundant organic components contributing to $PM_{2.5}$ (Qi et al., 2020). Different PAH diagnostic ratios are commonly used to investigate possible sources of PAHs, and subsequently, $PM_{2.5}$ (Dong et al., 2021; Gao and Ji, 2018; Yan et al., 2019). The Flt/(Flt + Pyr), BaA/(BaA + Chr) and Ant/(Ant + Phe) ratios were mostly higher than 0.50, 0.35 and 0.10, respectively, during the COVID-19 III period, revealing biomass and coal combustion, along with petroleum products, as the main source of $PM_{2.5}$ (Fig. 4a, b). This was expected, as activities vital to people's basic needs and the operation of the city, such as power generation and the production of certain essential materials, continued in lieu of social activities and transit (Zhao et al., 2020c). During the IV stage, the Flt/(Flt + Pyr) ratio varied was mostly > 0.50 (range: 0.50–0.64), while the Ant/(Ant + Phe) ratio was >0.10, which suggested biomass, coal, and petroleum combustion as a possible source of $PM_{2.5}$. During the same period, the BaA/(BaA + Chr) ratio was mostly > 0.35 (range: 0.31–0.37), while the IcdP/(IcdP + BghiP) ratio was <0.1. These ratios suggest a mixed source of $PM_{2.5}$ (vehicle emissions, biomass and coal combustion, and petroleum sources) during the IV stage, which can be attributed to increased traffic and the reopening of industries, especially the petrochemical industry. During stageV, the BaA/(BaA + Chr) ratio was mostly < 0.35, whereas the Ant/(Ant + Phe) was > 0.10, revealing petroleum combustion, especially vehicle exhaust and energy production from liquid fossil fuel and crude oil, as a source of $PM_{2.5}$. Our results reveal that the change in $PM_{2.5}$ composition was consistent with changes in traffic intensity. Since Guangzhou is characterized by light industry, $PM_{2.5}$ pollution from industrial sources is less severe than that in the BTH region (Wang et al., 2020; Zhao et al., 2020a). In northern China, stagnant airflow and uninterrupted emissions from power plants and petrochemical facilities contributed to severe haze formation (Le et al., 2020). Conversely, transportation sources should also contribute more to total $PM_{2.5}$ pollution in Guangzhou than what has been measured in other urban areas dominated by heavy industry. A similar study tracing the $PM_{2.5}$ pollution during the COVID lockdown in Hangzhou, a southern city in China, also revealed that reductions in vehicular emissions were more responsible for the $PM_{2.5}$ decline compared with stationary emissions (Liu et al., 2021). Therefore, traffic restrictions, which could be extensively studied during the COVID-19 lockdown, were effective at controlling $PM_{2.5}$ pollution in Guangzhou.

Interestingly, the COVID-19 outbreak included three distinct pandemic haze events (PEs), with $PM_{2.5}$ concentration peaks occurring on 11 February (PE-1), 15 March (PE-2), and 8 April (PE-3). We determined the chemical composition of $PM_{2.5}$ during these three PEs, corresponding to COVID III, IV, and V, respectively (Fig. 5). The contribution of EC to $PM_{2.5}$ ini-

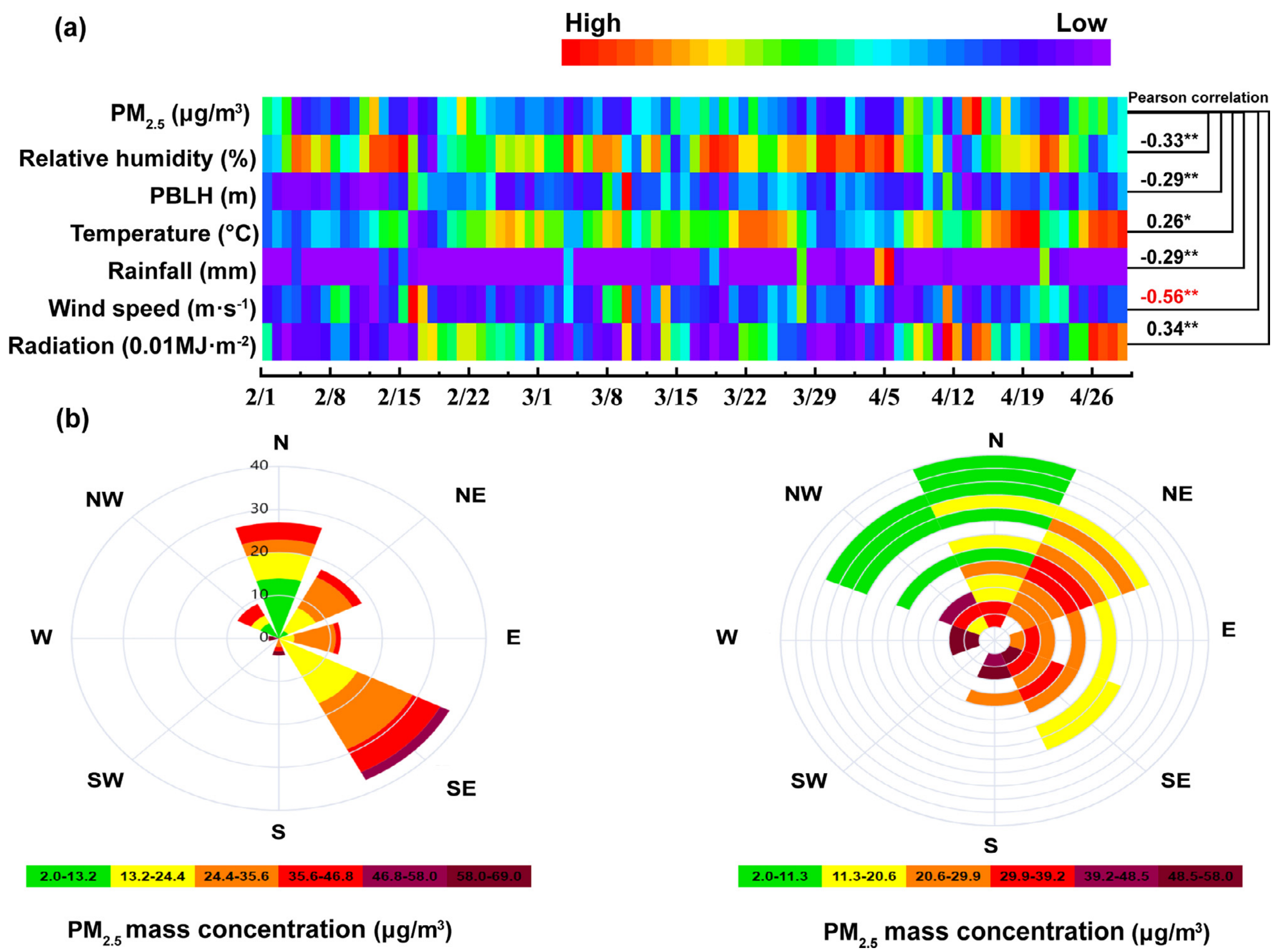

Fig. 3 – (a) The relationship between $PM_{2.5}$ pollution and meteorological elements during the COVID-19 lockdown in Guangzhou, (b) The frequency distributions of wind directions (Left) and speeds (Right) with $PM_{2.5}$ concentration (color demarcation) during the epidemic period of COVID-19. Wind speed: The wind speed represented by each grid increases progressively from the inside to the outside, increasing by 0.5 m/sec.

tially decreased and then increased from COVID-19 III to V. Since EC is formed by the inadequate combustion of carbon-based fuels, it can usually be used to identify primary emission sources (Wu et al., 2018). Therefore, the initial decrease in the share of EC in $PM_{2.5}$ indicates a decrease in primary sources of $PM_{2.5}$ during the lockdown periods. In addition, secondary pollutants (OC, SO_4^{2-}, NO_3^- and NH_4^+) were measured at especially high concentrations in comparison to the COVID-V period, suggesting that $PM_{2.5}$ pollution during the COVID-19 lockdown represented the enhanced formation of secondary aerosols with increased atmospheric oxidizing capacity. This is in agreement with previous research, as numerous studies have reported that the rapid formation of secondary inorganic aerosols was the main factor contributing to air pollution during the COVID-19 outbreak (Chang et al., 2020; Huang et al., 2021; Nichol et al., 2020).

The formation of haze is also strongly linked to the regional transportation of $PM_{2.5}$. To evaluate how regional transportation influences $PM_{2.5}$ pollution, a three-day back trajectory cluster analysis at 500 m was performed for each PEs, with the average $PM_{2.5}$ concentrations in the trajectory clusters shown in Table S10. The results revealed several transportation pathways for the studied PEs. The average $PM_{2.5}$ concentrations in two airflow trajectories entering Guangzhou from the northeast and southeast (Cluster 1 represents local emissions, while Cluster 2 represents marine transportation) are relatively high (36.5 $\mu g/m^3$, 36.3 $\mu g/m^3$), indicating that local sources significantly impacted $PM_{2.5}$ pollution in Guangzhou during COVID-19 period III (Fig. 4c). During the next period, air masses (Cluster 1 and Cluster 3) from the northwest, which passed over heavily polluted regions in northern and central China (e.g., Shanxi, Henan, and Anhui provinces), showed the highest $PM_{2.5}$ levels (37.3 $\mu g/m^3$) (Fig. 4d). This indicates that $PM_{2.5}$ pollution in Guangzhou was also affected by long-range transportation during the later stages of the COVID-19 lockdown. During phase V, air masses from the northeast of Guangzhou (Cluster 1), which represented the shortest inland trajectory, accounted for 50 % of total $PM_{2.5}$ pollution and also showed the highest average concentration of $PM_{2.5}$ (36.1 $\mu g/m^3$). Cluster 2 accounted for 25% of $PM_{2.5}$ pollution, with an average concentration of 31 $\mu g/m^3$ (Fig. 4e). Nevertheless, long inland trajectories from northeast China (Clus-

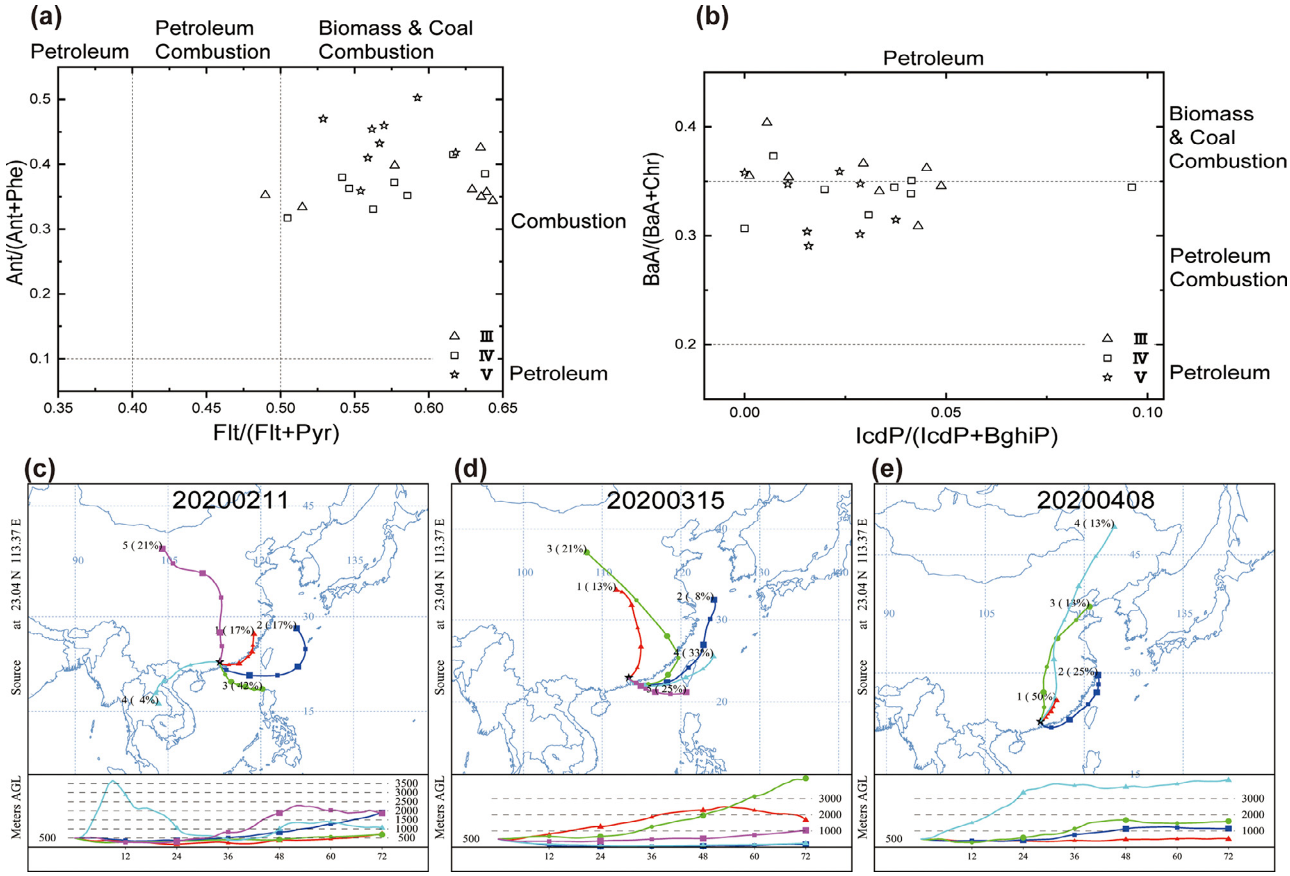

Fig. 4 – Cross plot for the PAH ratios of (a) Ant/(Ant + Phe) vs. Flt/(Flt + Pyr) and (b) BaA/(BaA + Chr) vs IcdP/(IcdP + BghiP), (c-e) Cluster analysis of air mass back trajectories during the COVID-19 lockdown.

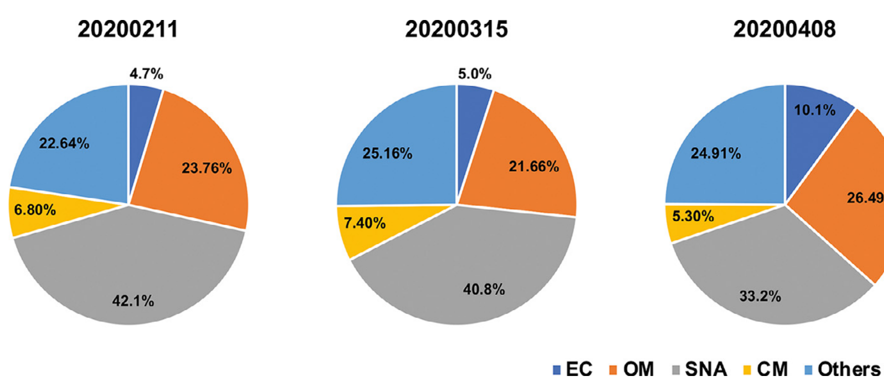

Fig. 5 – $PM_{2.5}$ concentration and composition of three pandemic haze events. OM (organic matter) = 1.6 ∗OC, EC: elemental carbon, SNA: sulfate, nitrate, and ammonium, CM (crustal elements) = 1.94 Ti + 2.2 Al + 1.63 Ca + 2.42 Fe + 2.49 Si, others = $PM_{2.5}$ mass–OM–EC–SNA–CM.

ters 3 and 4) account for a relatively low percentage (both 13%) and carry low average concentrations of $PM_{2.5}$ (21 $\mu g/m^3$, 17.7 $\mu g/m^3$). Hence, $PM_{2.5}$ pollution in Guangzhou mainly originated from local sources during the COVID-19 V period. The backward trajectory analysis showed that $PM_{2.5}$ pollution in Guangzhou mainly originated from local sources during period III and V, and resulted from long-distance transportation during stages IV. This corroborates what has been reported in other recent studies, i.e., local emissions and regional pollutant transportation most likely caused the pandemic haze events observed during the COVID-19 pandemic (Li et al., 2020; Shen et al., 2021; Zhao et al., 2020b).

We also studied the prevailing wind direction(s) to identify emission sources. The results revealed that: (1) southeasterly winds prevailed during the study period, while the westerly, southerly and southeasterly winds always showed high $PM_{2.5}$ concentrations; (2) most of the polluting industries (petrochemical industry and power plants) are located to the west, southerly and southeast of Guangzhou and its surrounding cities (Foshan, Zhaoqing, Dongguan and Huizhou) (Fig. S2). Based on these observations, it can be concluded that westerly, southerly and southeasterly winds will bring pollutants to Guangzhou and aggravate local $PM_{2.5}$ pollution. Therefore, controlling the emissions by these industries is of paramount importance to improving the air quality in Guangzhou.

3. Conclusions

Measurements taken during the COVID-19 lockdown show that $PM_{2.5}$ pollution in Guangzhou improved significantly as traffic and industrial emissions fell, with $PM_{2.5}$ levels below 6 $\mu g/m^3$ observed across five days of COVID-IV. These results indicate that controlling traffic and industrial emissions may be decisive for $PM_{2.5}$ pollution in Guangzhou; this is not the case for the BTH region and several cities in the Yangtze River Delta. Spatiotemporal analyses based on wind direction and $PM_{2.5}$ distribution indicate that decision-makers must also pay attention to $PM_{2.5}$ emissions originating from industrial areas to the south, southeast and west of Guangzhou, which can arrive by long-range transportation. The results also showed that a sharp decrease in primary $PM_{2.5}$ emissions can lead to an increase in the production of secondary particles, which - along with the long-distance transportation of particles - can offset the initial decrease in primary $PM_{2.5}$ emissions. Additionally, O_3 was the only atmospheric pollutant that demonstrated increased levels during COVID-19; hence, O_3 pollution will pose a challenge for Guangzhou and other regions in China. The present results confirm the effectiveness of previous $PM_{2.5}$ control measures in Guangdong Province, e.g., reducing coal combustion, construction site dust diffusion, and emissions linked to manufacturing, as well as installing monitoring equipment; on the other hand, the performed analyses also identified southeastern and western zones of Guangzhou as significant sources of $PM_{2.5}$. Moreover, the research highlights how ozone pollution can increase when $PM_{2.5}$ levels fall.

Acknowledgments

This work was supported by the National Natural Science Foundation of China (Nos. 21806025 and 91843301), the Natural Science Foundation of Guangdong Province (No. 2019A1515011294), the Science and Technology Planning Project of Guangdong Province (No. 2020B1212030008), the National Key Research and Development Project (No. 2019YFC1804604).

Appendix A Supplementary data

Supplementary material associated with this article can be found, in the online version, at doi:10.1016/j.jes.2021.07.009.

REFERENCES

An, Z., Huang, R.J., Zhang, R., Tie, X., Li, G., Cao, J., et al., 2019. Severe haze in northern China: a synergy of anthropogenic emissions and atmospheric processes. Proc. Natl. Acad. Sci. U.S.A. 116 (18), 8657–8666.

Bu, Q., Hong, Y., Tan, H., Liu, L., Wang, C., Zhu, J., et al., 2021. The modulation of meteorological parameters on surface $PM_{2.5}$ and O_3 concentrations in Guangzhou. China. Aerosol Air Qual. Res. 21 (1), 200084.

Chang, Y., Huang, R.J., Ge, X., Huang, X., Hu, J., Duan, Y., et al., 2020. Puzzling haze events in China during the Coronavirus (COVID-19) shutdown. Geophys. Res. Lett. 47 (12), 088533.

Chen, Y., Song, Y., Chen, Y.J., Zhang, Y., Li, R., Wang, Y., et al., 2020a. Contamination profiles and potential health risks of organophosphate flame retardants in PM2.5 from Guangzhou and Taiyuan, China. Environ. Int. 134, 105343.

Chen, Z., Chen, D., Zhao, C., Kwan, M.P., Cai, J., Zhuang, Y., et al., 2020b. Influence of meteorological conditions on $PM_{2.5}$ concentrations across China: a review of methodology and mechanism. Environ. Int. 139, 105558.

Chow, J.C., Watson, J.G., Chen, L.W.A., Chang, M.C.O., Robinson, N.F., Trimble, D., et al., 2007. The IMPROVE-A temperature protocol for thermal/optical carbon analysis: maintaining consistency with a long-term database. J. Air Waste Manag. Assoc. 57 (9), 1014–1023.

Dong, Z., Jiang, N., Zhang, R., Xu, Q., Ying, Q., Li, Q., et al., 2021. Molecular characteristics, source contributions, and exposure risks of polycyclic aromatic hydrocarbons in the core city of Central Plains Economic Region, China: insights from the variation of haze levels. Sci. Total Environ. 757, 143885.

Gao, Y., Ji, H., 2018. Characteristics of polycyclic aromatic hydrocarbons components in fine particle during heavy polluting phase of each season in urban Beijing. Chemosphere 212, 346–357.

Ghahremanloo, M., Lops, Y., Choi, Y., Mousavinezhad, S., 2021. Impact of the COVID-19 outbreak on air pollution levels in East Asia. Sci. Total Environ. 754, 142226.

Guangzhou Municipal Ecological Environment Bureau, G., China., 2020. Announcement of Guangzhou's environmental quality.

Guangzhou Statistics Bureau, G., China. 2020. Economic and social development statistical bulletin in 2019 (In Chinese).

Huang, R.J., Zhang, Y., Bozzetti, C., Ho, K.F., Cao, J.J., Han, Y., et al., 2014. High secondary aerosol contribution to particulate pollution during haze events in China. Nature 514 (7521), 218–222.

Huang, X., Ding, A., Gao, J., Zheng, B., Zhou, D., Qi, X., et al., 2021. Enhanced secondary pollution offset reduction of primary emissions during COVID-19 lockdown in China. Natl. Sci. Rev. 8 (2), 137.

Jia, H., Huo, J., Fu, Q., Duan, Y., Lin, Y., Jin, X., et al., 2020. Insights into chemical composition, abatement mechanisms and regional transport of atmospheric pollutants in the Yangtze River Delta region, China during the COVID-19 outbreak control period. Environ. Pollut. 267, 115612.

Le, T., Wang, Y., Liu, L., Yang, J., Yung, Y.L., Li, G., et al., 2020. Unexpected air pollution with marked emission reductions during the COVID-19 outbreak in China. Science 369 (6504), 702 -+.

Li, L., Li, Q., Huang, L., Wang, Q., Zhu, A., Xu, J., et al., 2020. Air quality changes during the COVID-19 lockdown over the Yangtze River Delta Region: an insight into the impact of human activity pattern changes on air pollution variation. Sci. Total Environ. 732, 139282.

Liao, X., Zou, T., Chen, M., Song, Y., Yang, C., Qiu, B., et al., 2021. Contamination profiles and health impact of benzothiazole and its derivatives in PM2.5 in typical Chinese cities. Sci. Total Environ. 755, 142617.

Liu, L., Zhang, J., Du, R., Teng, X., Hu, R., Yuan, Q., et al., 2021. Chemistry of atmospheric fine particles during the COVID-19 pandemic in a Megacity of Eastern China. Geophys. Res. Lett. 48 (2), 091611.

Liu, T., Wang, X., Hu, J., Wang, Q., An, J., Gong, K., et al., 2020. Driving forces of changes in air quality during the COVID-19 lockdown period in the Yangtze River Delta Region, China. Environ. Sci. Technol. Lett. 7 (11), 779–786.

Lu, H., Wang, S., Li, Y., Gong, H., Han, J., Wu, Z., et al., 2017. Seasonal variations and source apportionment of atmospheric PM2.5-bound polycyclic aromatic hydrocarbons in a mixed multi-function area of Hangzhou, China. Environ. Sci. Pollut. Res. 24 (19), 16195–16205.

Lv, Z., Wang, X., Deng, F., Ying, Q., Archibald, A.T., Jones, R.L., et al., 2020. Source-receptor relationship revealed by the halted traffic and aggravated haze in Beijing during the COVID-19 lockdown. Environ. Sci. Technol. 54 (24), 15660–15670.

Mousavinezhad, S., Choi, Y., Pouyaei, A., Ghahremanloo, M., Nelson, D.L., 2021. A comprehensive investigation of surface ozone pollution in China, 2015-2019: separating the contributions from meteorology and precursor emissions. Atmos. Res. 257, 105599.

Nichol, J.E., Bilal, M., Ali, M.A., Qiu, Z., 2020. Air pollution scenario over China during COVID-19. Remote Sens. 12 (13), 2100.

Qi, Z., Zhang, Y., Chen, Z.F., Yang, C., Song, Y., Liao, X., et al., 2020. Chemical identity and cardiovascular toxicity of hydrophobic organic components in PM2.5. Ecotoxicol. Environ. Saf. 201, 110827.

Shen, L., Zhao, T., Wang, H., Liu, J., Bai, Y., Kong, S., et al., 2021. Importance of meteorology in air pollution events during the city lockdown for COVID-19 in Hubei Province, Central China. Sci. Total Environ. 754, 142227.

Sun, Y., Chen, C., Zhang, Y., Xu, W., Zhou, L., Cheng, X., et al., 2016. Rapid formation and evolution of an extreme haze episode in Northern China during winter 2015. Sci. Rep. 6, 27151.

Tanzer-Gruener, R., Li, J., Eilenberg, S.R., Robinson, A.L., Presto, A.A., 2020. Impacts of modifiable factors on ambient air pollution: a case study of COVID-19 shutdowns. Environ. Sci. Technol. Lett. 7 (8), 554–559.

Wang, L., Li, M., Yu, S., Chen, X., Li, Z., Zhang, Y., et al., 2020. Unexpected rise of ozone in urban and rural areas, and sulfur dioxide in rural areas during the coronavirus city lockdown in Hangzhou, China: implications for air quality. Environ. Chem. Lett. 18, 1713–1723.

Wang, L., Liu, Z., Sun, Y., Ji, D., Wang, Y., 2015. Long-range transport and regional sources of PM2.5 in Beijing based on long-term observations from 2005 to 2010. Atmos. Res. 157, 37–48.

Wu, X., Vu, T.V., Shi, Z., Harrison, R.M., Liu, D., Cen, K., 2018. Characterization and source apportionment of carbonaceous PM2.5 particles in China - a review. Atmos. Environ. 189, 187–212.

Xu, K., Cui, K., Young, L.H., Hsieh, Y.K., Wang, Y.F., Zhang, J., et al., 2020a. Impact of the COVID-19 event on air quality in central China. Aerosol Air Qual. Res. 20 (5), 915–929.

Xu, Y., Xue, W., Lei, Y., Huang, Q., Zhao, Y., Cheng, S., et al., 2020b. Spatiotemporal variation in the impact of meteorological conditions on PM2.5 pollution in China from 2000 to 2017. Atmos. Environ. 223, 117215.

Yan, D., Wu, S., Zhou, S., Tong, G., Li, F., Wang, Y., et al., 2019. Characteristics, sources and health risk assessment of airborne particulate PAHs in Chinese cities: a review. Environ. Pollut. 248, 804–814.

Yin, C., Deng, X., Zou, Y., Solmon, F., Li, F., Deng, T., 2019. Trend analysis of surface ozone at suburban Guangzhou, China. Sci. Total Environ. 695, 133880.

Zhang, Y., Chen, Y., Li, R., Chen, W., Song, Y., Hu, D., et al., 2019. Determination of $PM_{2.5}$-bound polyaromatic hydrocarbons and their hydroxylated derivatives by atmospheric pressure gas chromatography-tandem mass spectrometry. Talanta 195, 757–763.

Zhao, N., Wang, G., Li, G., Lang, J., Zhang, H., 2020a. Air pollution episodes during the COVID-19 outbreak in the Beijing-Tianjin-Hebei region of China: an insight into the transport pathways and source distribution. Environ. Pollut. 267, 115617.

Zhao, X.J., Zhao, P.S., Xu, J., Meng, W., Pu, W.W., Dong, F., et al., 2013. Analysis of a winter regional haze event and its formation mechanism in the North China Plain. Atmos. Chem. Phys. 13 (11), 5685–5696.

Zhao, Y., Zhang, K., Xu, X., Shen, H., Zhu, X., Zhang, Y., et al., 2020b. Substantial changes in nitrogen dioxide and ozone after excluding meteorological impacts during the COVID-19 outbreak in Mainland China. Environ. Sci. Technol. Lett. 7 (6), 402–408.